

Crystallization of the PX domain of cytokine-independent survival kinase (CISK): improvement of crystal quality for X-ray diffraction with sodium malonate

Yi Xing^{a,b} and Wenqing Xu^{a*}^aDepartment of Biological Structure, University of Washington, Seattle, WA 98195, USA, and^bBiomolecular Structure and Design Program, University of Washington, Seattle, WA 98195, USACorrespondence e-mail:
wxu@u.washington.edu

Phox homology (PX) domains play critical roles in the intracellular localization of a variety of cell-signaling proteins through interactions with specific phosphoinositides. For cytokine-independent survival kinase (CISK), the PX domain also plays a role in the regulation of CISK activity in response to the activation of phosphatidylinositol-3 (PI-3) kinase. The PX domain of mouse CISK has been purified and crystallized, as well as its complex with a phosphoinositide ligand. The native PX domain was crystallized in space group *I4* and the crystals diffracted to a maximum resolution of 1.6 Å. Selenomethionine-derivatized PX domain was also prepared and crystallized for MAD phasing. In this study, the use of sodium malonate is the key to both successful crystallization and cryoprotection of the PX domain of CISK.

Received 24 April 2003

Accepted 14 July 2003

1. Introduction

The cellular level and the distribution of phosphoinositides, which determine the localization of many signaling proteins, are exquisitely regulated in cells in order to coordinate a wide range of cellular processes. The effects of phosphoinositides in cell regulation are primarily mediated through direct interactions with conserved phosphoinositide-binding domains (Fruman *et al.*, 1999; Leever *et al.*, 1999; Odorizzi *et al.*, 2000; Hurley & Meyer, 2001). The Phox homology domain (PX domain), a conserved structural motif containing about 120 residues, has been shown to interact with specific phosphoinositides (Sato *et al.*, 2001). Currently, more than 100 eukaryotic proteins have been found to be PX-domain-containing proteins, with a relatively low sequence conservation among the PX domains. These proteins function in cell growth and survival, cytoskeleton organization, membrane trafficking, T- and B-cell activation and neutrophil defense. PX-domain-regulated membrane targeting is a critical step in these important biological processes (Schultz *et al.*, 1998; Xu, Seet *et al.*, 2001).

Among the PX domain-containing proteins, cytokine-independent survival kinase (CISK) has been implicated as functioning in parallel with PKB/Akt in cell survival and insulin responses. CISK and Akt have a significantly homologous kinase domain and a C-terminal regulatory domain, but each of them has a different N-terminal membrane-targeting motif: a pleckstrin homology (PH) domain in Akt and a PX domain in CISK. In addition, both CISK and PKB/Akt are important downstream targets of phosphatidylinositol-3

(PI-3) kinase (Kobayashi & Cohen, 1999; Park *et al.*, 1999; Liu *et al.*, 2000). *In vivo*, PI-3 kinase generates a series of phospholipids *via* phosphorylation on the D-3 position of the inositol ring of phosphoinositides. These phospholipid products include phosphatidylinositol(3)P [PtdIns(3)P], PtdIns(3,4)P₂, PtdIns(3,5)P₂ and PtdIns(3,4,5)P₃. In the presence of these membrane-restricted messengers, signaling proteins with phosphoinositide-binding domains, such as PH, FYVE and PX domains, are targeted to the organelle membrane through protein–lipid interactions (Xu, Seet *et al.*, 2001). Localization of these proteins on the membrane initiates further downstream signaling events (Rameh & Cantley, 1999). As shown previously, both *in vitro* and *in vivo* the PX domain of CISK interacts preferentially with PtdIns(3,5)P₂ and PtdIns(3,4,5)P₃, which are responsible for targeting CISK to the endosomal compartments in response to PI-3 kinase signals. Disrupting the interaction between the CISK PX domain and phospholipids causes a decrease in CISK activity *in vivo* (Xu, Liu *et al.*, 2001).

Although CISK and Akt both utilize protein–lipid interactions in response to PI-3 kinase signals, these two pathways differ in many aspects. The CISK PX domain and the Akt PH domain have different preferences for phosphoinositides. Unlike the Akt PH domain, the CISK PX domain recognizes PtdIns(3,5)P₂ instead of PtdIns(3,4)P₂. This may explain the different subcellular localization of these two proteins. It has been shown that upon PI-3 kinase activation, Akt is translocated to and activated on the plasma membrane before being further transported into the nucleus (Andjelkovic *et al.*, 1997). However, CISK is

mostly found in the endosomal compartments and only rarely in the nucleus (Xu, Liu *et al.*, 2001). The specific preference for PtdIns(3,5)P₂ also implies unique functions of CISK that are different from those of Akt, such as the regulation of vesicle trafficking and certain membrane-protein sorting (Odorizzi *et al.*, 1998; Ikonov *et al.*, 2001).

Here, we report the crystallization and preliminary X-ray analysis of the CISK PX domain and its complex with PtdIns(3,5)P₂.

2. Methods and results

2.1. Expression and purification

A construct was made from the PGEX4T-1 plasmid (Pharmacia) encoding the gene for mouse CISK PX domain and a conserved linker between the PX domain and the kinase domain (residues 1–154, referred to hereafter as the 'PX domain'). Recombinant native PX domain and selenomethionine-derivatized PX domain (SeMet-PX) of CISK were both expressed as GST-fusion proteins in *Escherichia coli* cells with a thrombin-cleavage site after the GST tag.

For native protein expression, *E. coli* BL21(DE3) cells were cultured at 310 K in LB media until the OD₆₀₀ reached 0.4 before IPTG induction. The cells were spun down at 2000g after 4 h induction. The cell pellets were resuspended and sonicated in lysis buffer (phosphate-buffered saline con-

taining 0.1 mM PMSF, 0.2 mg ml⁻¹ benzamidine, 2 µg ml⁻¹ leupeptin, 2 µg ml⁻¹ pepstatin A, 0.2% Triton X-100, 0.2 mg ml⁻¹ lysozyme and 2 mM DTT). The cell lysates containing the GST fusion of native PX-domain protein (GST-PX) were clarified by centrifugation. GST fusion of SeMet-PX was expressed in the auxotrophic *E. coli* cell line B834 following a protocol originally designed for leaky protein expression (Doublé, 1997) and harvested in the same way as the native protein.

Purification of both native PX and SeMet-PX was carried out using the same procedure. Filtered supernatant from the cell lysates was loaded onto glutathione-affinity resin (Pharmacia). The affinity resin was washed sequentially with three bed volumes of wash buffer A (50 mM Tris pH 8.5, 0.5 M NaCl, 0.5% Triton X-100, 2 mM DTT) and two bed volumes of wash buffer B (50 mM Tris pH 8.5, 0.1 M NaCl, 2 mM DTT). GST-PX was then eluted from the resin with three bed volumes of elution buffer (100 mM Tris pH 8.5, 0.1 M NaCl, 20 mM reduced glutathione, 2 mM DTT). The elution fractions were dialyzed into thrombin-cleavage buffer (50 mM Tris pH 8.5, 50 mM NaCl, 2 mM DTT). After thrombin (Pharmacia) cleavage, conducted at 293 K, the protein solution was loaded back onto glutathione-affinity resin to remove GST and uncleaved GST fusion proteins. The flowthrough from the affinity resin was collected and analyzed by SDS-PAGE (Fig. 1, lane 2). A major contaminant was removed by applying the protein sample to a Q-Sepharose HP column (Pharmacia). The Q-Sepharose HP column flowthrough, which mainly contained the PX-domain protein, was collected and loaded onto an SP-Sepharose HP column (Pharmacia) equilibrated in column buffer A (20 mM Tris pH 7.5, 25 mM NaCl, 2 mM DTT). The PX-domain protein was further purified on the

SP-Sepharose HP column using a linear salt gradient from column buffer A to column buffer B (20 mM Tris pH 7.5, 1 M NaCl, 2 mM DTT). The elution fractions containing the PX-domain protein from a single peak were analyzed by SDS-PAGE and pooled together (Fig. 1, lane 3). The purified PX domain protein pool was finally concentrated to 15 mg ml⁻¹ for native PX and 12 mg ml⁻¹ for SeMet-PX in storage buffer (20 mM Tris pH 7.5, 50 mM NaCl, 2 mM DTT).

Dynamic light scattering (DynPro99; Protein Solutions, Inc.) was used to analyze the solution properties of native PX-domain protein at 15 mg ml⁻¹ in storage buffer (20 mM Tris pH 7.5, 50 mM NaCl, 2 mM DTT). The result disclosed a monodispersive profile with a molecular weight of ~34 kDa, corresponding to a PX-domain dimer. This result suggests that the PX domain dimerizes in the storage buffer. It is consistent with a yeast two-hybrid screen, which also suggests that the PX domain of CISK can form a homodimer or homooligomers (Songyang, 2002). It would be interesting to understand the structural basis of PX-domain dimerization.

2.2. Crystallization

Native PX-domain crystals initially appeared as microcrystals at 293 K in a hanging drop containing 1 µl 15 mg ml⁻¹ protein stock and 1 µl reservoir solution [0.1 M sodium citrate pH 5.6, 2.5 M (NH₄)₂SO₄, 10 mM DTT] in 15–20 d from a screening kit prepared in our laboratory. After optimization, bipyramidal crystals grew from a hanging drop with a 1:2 volume ratio of 15 mg ml⁻¹ protein stock and reservoir solution [0.1 M sodium citrate pH 5.8, 2.0 M (NH₄)₂SO₄] in about 10 d (Fig. 2a). Removing the reducing reagent DTT seems critical to crystal growth after nucleation,

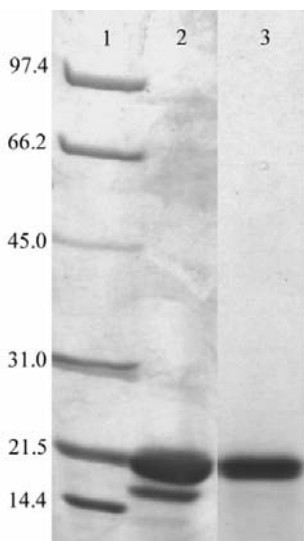


Figure 1
SDS-PAGE analysis of the CISK PX-domain purification. Lane 1, molecular-weight markers in kDa. Lane 2, partially purified native PX domain. The upper band is the PX domain and the lower band is a major contaminant. Lane 3, purified native PX domain.

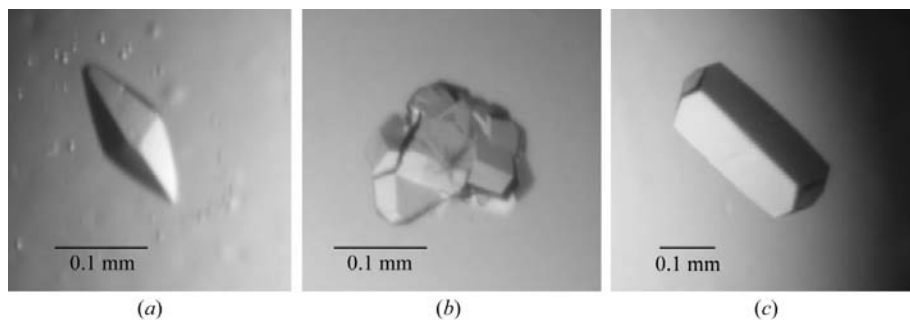


Figure 2
(a) A single crystal of native PX domain grown from 0.1 M sodium citrate pH 5.8 and 2.0 M (NH₄)₂SO₄, approximately 0.2 mm in the longest dimension. (b) Clustered SeMet-PX crystals grown from 0.1 M sodium citrate pH 5.8 and 2.0 M (NH₄)₂SO₄. (c) A crystal of SeMet-PX grown from 0.1 M sodium citrate pH 5.8 and 2.0 M sodium malonate pH 5.8 with maximum dimensions of 0.3 × 0.1 × 0.1 mm.

Table 1

The native PX domain and the PX–Di-C₄PtdIns(3,5)P₂ complex crystal data-set statistics.

Values in parentheses refer to the outer-shell bin.

	Native PX	PX–Di-C ₄ PtdIns(3,5)P ₂
Space group	<i>I4</i>	<i>I4</i>
Unit-cell parameters (Å)	<i>a</i> = <i>b</i> = 74.9, <i>c</i> = 51.7	<i>a</i> = <i>b</i> = 74.6, <i>c</i> = 51.6
Resolution limits (Å)	50.0–1.60 (1.66–1.60)	50.0–2.40 (2.49–2.40)
Total reflections	100739	17928
Unique reflections	18760	5492
Redundancy	5.4	3.3
Completeness (%)	98.6 (97.7)	97.4 (96.4)
Average <i>I</i> σ(<i>I</i>)	34.0 (6.5)	15.7 (5.0)
<i>R</i> _{merge} † (%)	4.0 (19.9)	6.7 (16.8)
Mosaicity (°)	0.2	0.8

† $R_{\text{merge}} = 100 \sum |I_i - \langle I \rangle| / \sum I_i$, where I_i is the intensity of the i th observation.

although a dissolved native PX-domain crystal appears as an 18 kDa (monomer) single band in the non-reducing SDS–PAGE.

The PX–phosphoinositide complex was also prepared by mixing the native PX-domain protein stock solution and a solution of Di-C₄PtdIns(3,5)P₂ (Echelon, Utah) in water at a final protein concentration of 12 mg ml⁻¹ and a Di-C₄PtdIns(3,5)P₂ concentration of 2 mM. Both PX–Di-C₄PtdIns(3,5)P₂ and SeMet-PX crystals grew under similar conditions as for the unliganded native PX domain.

There were common problems with the PX-domain crystals when (NH₄)₂SO₄ was used as the precipitant. For native PX and the PX–Di-C₄PtdIns(3,5)P₂ complex, single crystals were only reproducible in 1% of the drops. These crystals were very sensitive to air and the externally added cryosolution when we tried to freeze them. X-ray analysis showed that PX-domain crystals grown from (NH₄)₂SO₄ diffracted very weakly. The SeMet-PX crystals produced in (NH₄)₂SO₄ were all severely clustered and unsuitable for data collection (Fig. 2b).

Previously, sodium malonate has been shown to be the most effective salt in crystallizing macromolecules compared with 11 other salts (McPherson, 2001). In the case of PX-domain crystallization, sodium malonate was found to be a better precipitant than (NH₄)₂SO₄ for all the PX-domain crystals.

Single crystals of native PX, PX–Di-C₄PtdIns(3,5)P₂ and SeMet-PX, grown in about 10 d with similar shapes, were all highly reproducible in hanging drops with a reservoir solution consisting of 0.1 M sodium citrate pH 5.5–5.8 and 2.0 M sodium malonate buffered to pH 5.5–5.8 (Fig. 2c). Not only did sodium malonate dramatically increase the reproducibility of single PX-domain crystals, but it also acted as a good cryoprotectant. Crystals grown from 2.0 M sodium malonate were already cryoprotected. These crystals were flash-frozen with liquid nitrogen directly from the crystallization drop for data collection. Compared with those grown from (NH₄)₂SO₄, crystals grown from sodium malonate were much more resistant to physicochemical shocks during the freezing procedure. PX-domain crystals produced in sodium malonate diffracted strongly and were used for data collection.

2.3. Data collection and analysis

Data sets of both native PX and PX–Di-C₄PtdIns(3,5)P₂ crystals were collected on beamline 19BM at the Advanced Photon Source (APS) using a 3k × 3k CCD detector (ANL-ECT). One native PX crystal diffracted to 1.6 Å. PX–Di-C₄PtdIns(3,5)P₂ crystals diffracted to about 2.4 Å with a much higher mosaicity than the native crystals. The data sets were processed and scaled with *DENZO/SCALEPACK* (Otwinowski & Minor, 1997). Statistics for both data sets are given in Table 1. The native PX crystal belongs to space group *I4*, with unit-cell parameters *a* = *b* = 74.95, *c* = 51.70 Å. Given a molecular weight of 17.9 kDa for the protein, a single PX-domain molecule per asymmetric unit results in a Matthews coefficient of 2.0 Å³ Da⁻¹, with a solvent content of 33.4% (Matthews, 1968). Molecular replacement with available PX-domain crystal structures (Bravo *et al.*, 2001; Karathanassis *et al.*, 2002) did not yield an

obvious solution. Collection of a selenomethionine MAD data set is currently under way.

We thank Drs D. Liu and Z. Songyang for the mouse CISK PX-domain expression vector and Dr R. Zhang for assistance with data collection at the Advanced Photon Source (APS).

References

- Andjelkovic, M., Alessi, D. R., Meier, R., Fernandez, A., Lamb, N. J., Frech, M., Cron, P., Cohen, P., Lucocq, J. M. & Hemmings, B. A. (1997). *J. Biol. Chem.* **272**, 31515–31524.
- Bravo, J., Karathanassis, D., Pacold, C. M., Pacold, M. E., Ellison, C. D., Anderson, K. E., Butler, P. J. G., Lavenir, I., Perisic, O., Hawkins, P. T., Stephens, L. & Williams, R. L. (2001). *Mol. Cell.* **8**, 829–839.
- Doublé, S. (1997). *Methods Enzymol.* **276**, 523–530.
- Fruman, D. A., Rameh, L. E. & Cantley, L. C. (1999). *Cell.* **97**, 817–820.
- Hurley, J. H. & Meyer, T. (2001). *Curr. Opin. Cell Biol.* **13**, 146–152.
- Ikonomov, O. C., Sbrissa, D. & Shisheva, A. (2001). *J. Biol. Chem.* **276**, 26141–26147.
- Karathanassis, D., Stahelin, R. V., Bravo, J., Perisic, O., Pacold, C. M., Cho, W. & Williams, R. L. (2002). *EMBO J.* **21**, 5057–5068.
- Kobayashi, T. & Cohen, P. (1999). *Biochem. J.* **339**, 319–328.
- Leevers, S. J., Vanhaesebroeck, B. & Waterfield, M. D. (1999). *Curr. Opin. Cell Biol.* **11**, 219–225.
- Liu, D., Yang, X. & Songyang, Z. (2000). *Curr. Biol.* **10**, 1233–1236.
- McPherson, A. (2001). *Protein Sci.* **10**, 418–422.
- Matthews, B. W. (1968). *J. Mol. Biol.* **33**, 491–497.
- Odorizzi, G., Babst, M. & Emr, S. D. (1998). *Cell.* **95**, 847–858.
- Odorizzi, G., Babst, M. & Emr, S. D. (2000). *Trends Biochem. Sci.* **25**, 229–235.
- Otwinowski, Z. & Minor, W. (1997). *Methods Enzymol.* **276**, 307–326.
- Park, J., Leong, M. L., Buse, P., Maiyar, A. C., Firestone, G. L. & Hemmings, B. A. (1999). *EMBO J.* **18**, 3024–303.
- Rameh, L. E. & Cantley, L. C. (1999). *J. Biol. Chem.* **274**, 8347–8350.
- Sato, T. K., Overduin, M. & Emr, S. D. (2001). *Science*, **294**, 1881–1885.
- Schultz, J., Milpetz, F., Bork, P. & Ponting, C. P. (1998). *Proc. Natl Acad. Sci. USA*, **95**, 5857–5864.
- Songyang, Z. (2002). Personal communication.
- Xu, J., Liu, D., Gill, G. & Songyang, Z. (2001). *J. Cell Biol.* **154**, 699–705.
- Xu, Y., Seet, L. F., Hanson, B. & Hong, W. (2001). *Biochem. J.* **360**, 513–530.